Develop End-to-End Anomaly Detection System

Emanuele Mengoli
École Polytechnique
Paris, France
em.mengoli@gmail.com

Zhiyuan Yao
Cisco Meraki
Paris, France
yzhiyuan@cisco.com

Wutao Wei
Cisco Meraki
San Francisco, USA
wutwei@cisco.com

arXiv:2402.10085v1 [cs.NI] 1 Feb 2024

Abstract—Anomaly detection plays a crucial role in ensuring network robustness. However, implementing intelligent alerting systems becomes a challenge when considering scenarios in which anomalies can be caused by both malicious and non-malicious events, leading to the difficulty of determining anomaly patterns. The lack of labeled data in the computer networking domain further exacerbates this issue, impeding the development of robust models capable of handling real-world scenarios. To address this challenge, in this paper, we propose an end-to-end anomaly detection model development pipeline. This framework makes it possible to consume user feedback and enable continuous user-centric model performance evaluation and optimization. We demonstrate the efficacy of the framework by way of introducing and bench-marking a new forecasting model – named *Lachesis* – on a real-world networking problem. Experiments have demonstrated the robustness and effectiveness of the two proposed versions of *Lachesis* compared with other models proposed in the literature. Our findings underscore the potential for improving the performance of data-driven products over their life cycles through a harmonized integration of user feedback and iterative development.

Index Terms—Anomaly Detection, Particle Filter, Prediction, Human Feedback

I. INTRODUCTION

Anomaly detection systems are a category of purpose-built techniques designed to predict and prevent abnormal occurrences within complex systems through continuous real-time monitoring [1], [2]. These systems have the ability to anticipate upcoming data values, thereby facilitating informed decision making. In the context of networking, the indispens-ability of such systems is underscored by their pivotal role in performing network health management functions, thereby ensuring seamless operational continuity [3].

The focus of these models lies in the domain of prediction execution, which involves determining an appropriate threshold for triggering alerts [4]. This paper is situated within this domain and focuses its attention on the issue of anomalies related to system performance. Our endeavour extends the groundwork established in [3], with a particular emphasis on the use of supervised techniques for the detection and identification of anomalies in the computer networking domain.

It is noteworthy that these systems often lack to identify the root cause of anomalous events. While identifying and

quantifying responsibility for mono-causal events can be a straightforward exercise, the complexity of the task increases significantly when faced with scenarios involving multiple causal factors. The identification of anomaly causation is of great interest to users and network operators. In particular, supervised methods require the availability of anomaly ground truth data to establish causal responsibilities.

In this paper, we present a modularized framework that allows continuously evaluating and optimizing a supervised anomaly detection model. The foundation and the demonstration of our framework is anchored in the context of predicting abnormally high amount of networking event occurrences in networking switches developed by Cisco Meraki.

The development of an anomaly detection system with the ability to continuously quantify the responsibility of potential root causes presents a number of challenges.

Challenge 1: Extensible Labelled Data Acquisition. The construction and fine-tuning of anomaly detection systems are fundamentally grounded in the availability of a substantial and well-labeled dataset. However, achieving this foundation is met with intrinsic challenges owing to the multifaceted nature of networking systems. We tackle this challenge by introducing an adaptive and extensible predictive model that can evolve in tandem with the network it monitors, thereby sustaining a relevant and acute predictive capability through the incorporation of user feedback loops.

Challenge 2: Accuracy - Responsiveness trade-off. There is a delicate balance between accuracy and real-time re-sponsiveness. Achieving high predictive accuracy is an ulti-mate goal in developing anomaly detection systems, yet the increased latency introduced by substantial models impairs the timely identification and mitigation of anomalies. Our proposed algorithm achieves a synthesis of these attributes by combining two proposed versions of the time-series models. The first prioritises accuracy in the prediction phase, followed by a second version adapted to real-time implementation. The latter is designed to adapt predictions based on the degree of data deviation from the training time series.

Challenge 3: Scalability. The expansive and ever-growing network infrastructures dictate a prerequisite for the anomaly detection system to exhibit a high degree of scalability. Effec-tive deployment requires that the models are able to deliver tailored performance with inherent flexibility. Maintaining

scalability should be intrinsic to both the initial development and the ongoing maintenance of the system, ensuring not only a reactive adaptability to current network configurations but also a proactive readiness to accommodate future growth and complexities with minimal disruptions.

The structure of the paper is as follows: Section II provides a literature review over related anomaly detection systems. Section III describes the essential background information on the problem in which we demonstrate our proposed solution, and formulates the problem to solve. The designed framework and the proposed algorithm is explained in Section IV. Subsections IV-C to IV-D detail specific components of the proposed anomaly detection model. The evaluation process is described in Section V. Finally, concluding remarks are presented in Section VI.

II. Related work

The literature landscape revealed a substantial body of work on anomaly detection, focusing mainly on network intrusions rather than performance anomalies. However, common tools are used to detect anomalous behaviours, namely supervised and unsupervised techniques, so a literature review was conducted on these techniques.

Unsupervised techniques demonstrated the ability to effectively detect anomalous patterns. However, their sensitivity to significant fluctuations in the data made it difficult to distinguish between normal and anomalous patterns [5]. Empirical evidence highlighted the superior performance of supervised learning over unsupervised methods, provided that the test data did not contain unknown attacks [4]. In the context of real-time implementation, supervised techniques were preferred due to their less resource-intensive testing phase [5].

As shown in [6], Ericsson Lab has proposed a customised analytical engine for anomaly detection in mobile networks. This solution employs an Autoregressive Integrated Moving Average (ARIMA) model to predict Key Performance Indicator (KPI) values and a heuristic algorithm to calculate the actual value as ground truth. This approach is particularly suitable for scenarios with low data volatility; however, in cases of greater fluctuation, reliance on labelled data becomes essential to accurately distinguish normal from abnormal behaviour and to avoid estimation errors.

An unsupervised algorithm based on Isolation Forest (iForest) has been proposed for anomaly classification in [7]. While this approach showed robustness under the assumption of stationarity or periodicity of the time series, it may lack precision in the presence of high data volatility. In such cases, labelled truth data are essential to build accurate anomaly models.

Furthermore, [8] introduced an unsupervised spatio-temporal anomaly detector consisting of two stages: geographical anomaly identification and temporal anomaly detection. This system excelled in detecting anomalous behaviour related to geographical location and time, thus addressing the need for timely intervention to maintain network resilience and service

availability. Using One Class SVM (OCSVM), Long Short-Term Memory (LSTM) and Support Vector Regression (SVR) recurrent neural networks, this approach outperformed iForest and ARIMA in spatial and temporal detection, respectively.

Authors in [9] proposed a model that requires a set of previously labelled data to train the semi-supervised root cause analysis, leading to a classification problem centred on matching the root cause, using a random forest classifier. Pre-labelled data may be complex to obtain since it requires full knowledge of the system dynamics. This could be extremely challenging to achieve, especially in a scenario that is characterized by multiple causes, for which specific responsibility is hard to define or quantify, as in our scenario.

The authors of [10] proposed an unsupervised method of inferring root causes in mobile networks using finite state machines (FSM) based on Principal Component Analysis (PCA), which reduces dimensionality and extracts meaningful data from the original dataset. FSM identifies problematic procedures that result in cascading failures in subsequent procedures. The identification of the specific problem is made possible by translating the error codes of the procedures once the original anomalous pattern is identified. The results of FSM are intriguing when applied to a time series or dataset with moderate-sized normal and anomalous patterns, such as a specific messages sequence shown in [10]. However, this method is combinatorial in nature. As a result, the complexity is likely to increase considerably when considering the stochastic nature of normal and abnormal patterns.

In [11], the authors proposed an unsupervised model built in two-stage clustering and further improved by applying transfer learning to historical data. This system requires a deterministic pass/fail classifier to detect anomalous behaviour in the data samples. Achieving this can be difficult if normal patterns follow stochastic behaviour.

An autonomous diagnostic system within a self-healing network is proposed in [12]. It uses a self-organising map (SOM) to generate clusters. Expert-based labelling is performed on the clusters, guided by their statistical characteristics.

Unlike prior studies, this paper proposes a simple yet effective model development pipeline that allows continuously develop and optimize user-centric anomaly detecting systems in an extensible manner. Given the focus of this paper on high-fluctuation data exhibiting pattern similarities between malicious and non-malicious causes, it is preferred to use a supervised method supported by labelled ground truth data. Furthermore, the unique statistical and temporal properties associated with each node introduced challenges to classical supervised approaches. In light of these considerations, we had introduced *Lachesis*, a particle-filter-based anomaly detection algorithm. To the authors knowledge no particle-filter-based anomaly detection system for network management has been proposed in the literature to date. To assess the forecasting accuracy and performance of our proposed model, we had conducted a comparative analysis with the following algorithms: Prophet [13], [14], statistical model [3] (named phase 1 for the purpose of this paper), Dynamic Linear Model

(DLM) [15], [16], Autoregressive Integrated Moving Average (ARIMA) [17], [18], Seasonal Autoregressive Integrated Moving Average (SARIMA) [17], [19], linear and quadratic regression [20], [21].

III. PROBLEM FORMULATION

In this paper, we exemplifies the model development pipeline for anomaly detection system development in the context of a typical event in networking switches. In particular, we focus on Layer-2 address flapping detection, commonly referred as Media Access Control (MAC) flapping detection. For consistency with the nomenclature, we will use the term MAC-flap detection when referring to this type of event.

MAC-flap event occurs when a MAC address is learned 3 times or more on 2 or more different ports within 10 seconds on a networking switch [22]. MAC-flap events can cause packet loss in the network. Meraki switches include MAC-flap detection as a standard feature, which monitors the MAC forwarding table and reports flap events on the dashboard, as shown in Figure 2. However, switches do not have a built-in intelligence mechanism that triggers detection only in response to real problems. As a result, this alerting system can be overwhelmed by both true and false positives, generating noise to the end users. At the mean time, the root causes of MAC-flapping are not intuitive. This problem particularly affects the troubleshooting activity of network administrators, as the burst visibility affects the identification of the root cause of anomalies.

The goal of building an intelligent alert system is to help identify a baseline for each networking switch and trigger an alert only when the amount of MAC-flap events surpasses the derived baseline. This process can be abstracted as a time-series forecasting problem, *i.e.*, given the past 5 weeks' historical data of the number of MAC-flap events, we want to predict the next week's MAC-flap events for each node. Then the second step is to identify whether the generated alerts correspond to actual networking issues in the network, based on which we can evaluate the alert accuracy.

IV. METHODOLOGY

To tackle this real-world networking problem and its corresponding challenges, we propose a model development framework, accompanied by a particle-filter-based alerting system (named *Lachesis*). They are orchestrated to minimise false positive alerts, allowing further investigation of potential root causes and to determine the share of responsibility. Lachesis learns from the historical data to generate a baseline. It forecasts future data values and predicts an upper-bound on the number of MAC-flap events in a given time window, above which an alarm is triggered. The model development pipeline then allows to iteratively and continuously benchmarking and optimizing the alerting systems using various data-driven methods.

A. Model Development Pipeline

An automated pipeline is a cornerstone in orchestrating scalable, extensible, reproducible, and efficient model development. We propose a model development pipeline depicted in Figure 1, which not only lays down a robust blueprint for ML operations but transcends into a facilitator for a refined user experience through the incorporation of user feedback.

User feedback emerges as a cardinal element, steering the evolvement of the system through enriched labeled data procurement and user experience enhancement. Networking systems are characterized by dynamic state transitions that not only occur at large scales but also transpire rapidly, often outpacing the ability of existing systems to identify and tag them appropriately. Moreover, the underlying triggers of anomalous events are diversified, emanating from a range of factors including diverse protocol implementations and their respective versions. At the mean time, when developing data-driven models, it is important to take user experience into account and align user expectation and requirements with our data-driven products. Our proposed pipeline is able to resolve this by incrementally absorbing user feedback in an extensible manner.

The proposed pipeline (Figure 1) comprises 6 components unified to engender a data-driven solution for forecasting and generating alerts pertinent to the anomaly detection system outlined in this paper. Each component is designed to bring a seamless transition from data procurement to user feedback integration, anchoring on a symbiotic relationship between the system and its users to facilitate continuous improvement through iterative learning and feedback assimilation.

1) Data Management: This component is responsible for extracting and validating data obtained from diverse sources. These processes are orchestrated in a structured data warehouse. We expound on the measures adopted to validate the extracted data, fostering a repository enriched with credible and quality data, which forms the bedrock for feature management and model training.

2) Feature Management: This component is responsible for preparing the raw data into a format ready for feature extraction, as well as the transformation of prepared data into features that are conducive for the model learning process. Making this component independent helps control the versions of input data for various models, meanwhile, facilitate feature selection and extraction.

3) Experiment Management: On the heart of the pipeline, this component is responsible for model training and inference. It offers the flexibility in accommodating iterative learning through checkpoints and retraining, ensuring a progressive model evolution. Besides model checkpoints and predictions generated by the models, we also track and evaluate the computational complexity of the model.

4) Evaluation Management: This component is separated from the experiments managed above so that jobs can be scheduled in parallel. Decoupling the evaluation also allows for seamlessly updating evaluation metrics without re-running heavy jobs of experiments (model training and inferring). In
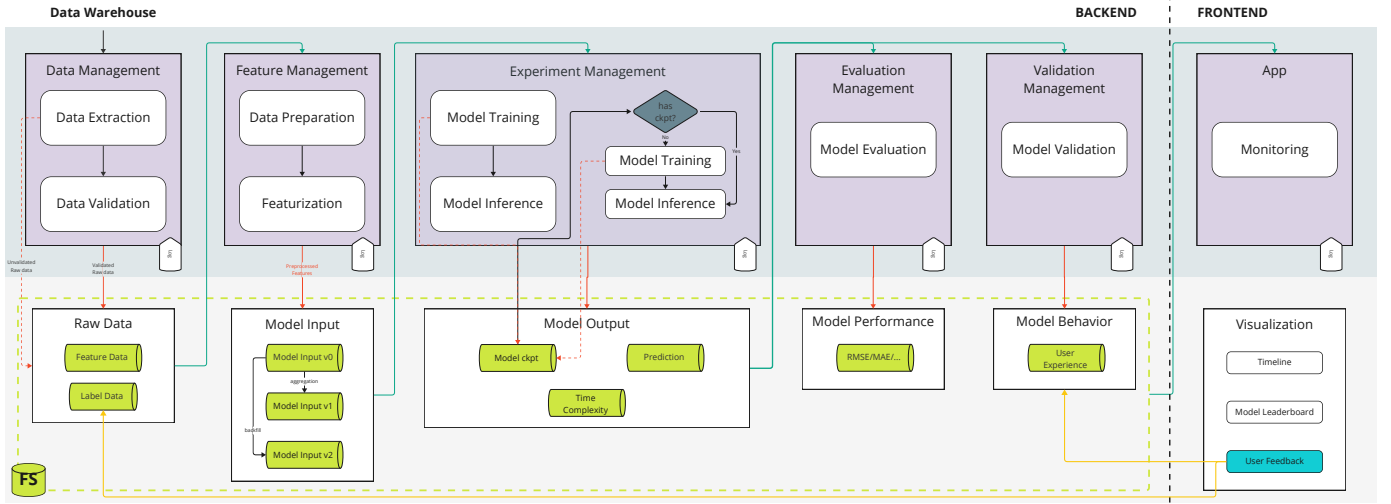
Fig. 1. Model development lifecycle taking user feedback into the loop.

Fig. 2. MAC-flap detection.

the context of MAC-flap alerting systems, MAE, MSE, and RMSE are utilized in gauging the model's forecasting prowess.

5) Validation Management: This key component bridges the technical finesse of the model and the practical business requirements and user experiences. Besides the technical evaluation mentioned above, it is imperative to ensure that the developed model aligns well with the broader business objectives. The most significant objective of customer-facing data-driven products is dedicated to analyzing and integrating user feedback to create a model that is responsive to the user's requirements and preferences. We create a channel for users feedback on various facets such as false positives/negatives, alert sensitivities, and other experiential aspects. By assimilating this direct feedback from end-users, we enrich the validation process, improving user satisfaction metrics and operational efficiency.

6) Frontend Application: The frontend application is the user-facing component of our framework, designed to be an interactive platform where users can engage directly with the system. It gives insights into the various performance indicators and presents a graphical representation of the forecasting timelines, allowing users and stakeholders to visualize the efficacy of the alerting system over periods. The frontend application provides a two-way communication channel, allowing users to provide feedback on the forecasting and alert generation process directly. Moreover, this interface enables continuous learning, as it facilitates the collection of labeled data through user feedback, thereby integrating an incremental improvement in the model's accuracy.

Whilst the potential root causes of MAC-flap events vary across different networking setups, this paper focuses on one

TABLE I Evaluation and Validation Metrics

Metric	Description
Evaluation (Regression)	
MSE	Mean Squared Error
RMSE	Root Mean Squared Error
MAE	Mean Absolute Error
Computational Complexity	
t_{train} (s) / 1k data points	Time for training per 1k data points
t_{infer} (s) / 1k data points	Time for inference per 1k data points
t_{train} (s) / 1k nodes	Time for training per 1k nodes
t_{infer} (s) / 1k nodes	Time for inference per 1k nodes
Validation (User Experience)	
Avg. Daily Alerted Nodes	Average number of nodes alerted per day
Avg. Daily Alerts	Average number of alerts per day
Total Alerts	Total alerts in whole prediction time-span
Avg. Alert Duration (min.)	Average alert duration
Std. Alert Duration (min.)	Standard deviation alert duration
Avg. Alerts per hour	Average alerts per hour
Std. Alerts per hour	Standard deviation alerts per hour
Accuracy	$\frac{TP+TN}{\text{Total}}$
Precision	$\frac{TP}{TP+FP}$
Recall	$\frac{TP}{TP+FN}$
Specificity	$\frac{TN}{TN+FP}$
Balanced Accuracy	$\frac{\text{Recall}+\text{Specificity}}{2}$

root cause identified via this model development pipeline – switch network loop [22]. Network loops occur when a switch detects its own MAC address on a received loop detection control packet [22]. This can be avoided by activating the *Spanning Tree Protocol (STP)* function which determines the

		Actual Networking Issue	
		Positive	Negative
Alert	Positive	True Positive (TP)	False Positive (FP)
	Negative	False Negative (FN)	True Negative (TN)

Fig. 3. Confusion matrix of MAC-flap alerts.

active ports among the switches of the topology [23]. The whole list of evaluation and validation metrics covered by the pipeline throughout all the components is summarized in Table I. Model evaluation is conducted with 3 regression metrics. Computational complexity is assessed over both the number of time-series data points and number of nodes (network switches). Model validation is based on user experience. We measure the alert frequencies and ratio so as to consolidate whether the alerts become noisy for the end-users. Besides, we assess the accuracy of the alerts based on the confusion matrix depicted in Figure 3, *e.g.* if an alert is raised for a node within 1 hour difference to when an actual networking issue (*i.e.*a network loop is detected), the alert is classified as a true positive.

B. Lachesis Model

To tackle the time-series forecasting problem for MAC-flap events, 2 versions of the predicting model Lachesis are proposed and assessed with the proposed pipeline. The underlying intuition of Lachesis is that anomalies of MAC-flap events can result from non-malicious causes, such as client roaming across multiple access points, recurring consistently on the same day of the week and at the same time. Conversely, it links malicious anomalies to sporadic events occurrences. Predictions are made for each node given the time series data of timestamps and respective number of MAC-flap events, from which weekday dw and time t are then extrapolated.

C. Lachesis version 0

The first version of the Lachesis model takes five weeks of historical data, and then makes predictions for the sixth week.

The user must specify the time aggregation parameter and the granularity in order to divide the series into a succession of discrete signals in the time domain.

In our case, a time aggregation of 1 hour is considered, with granularity to the minute. The user sets the forecast flag η, deciding whether to run a forecast or an upper-bound estimation.

The time of day is used to set the beginning of the time bucket obtained by grouping the time series on a daily basis and according to the time aggregation parameter τ. After grouping the input time series by date and time of day, each signal is transformed into the frequency domain using the Fast

Fourier Transform (FFT) [24], resulting in a discrete frequency transform of the data Z_k. The frequency domain is used both to reduce the size of the dataset and to improve the visibility of recursive values.

By grouping these values by day of the week and time slot (dw, t_τ), a significant value is obtained for each frequency κ through the application of a custom lambda function:

$$\tilde{Z}_\kappa = \lambda(Z_\kappa)^{dw, t_\tau} =$$
$$= \left[\left(\sqrt{\hat{Z}_k} \cdot |\bar{Z}_k + 3\sigma| \right) + \sqrt{\text{card}(Z_k)} \right] \cdot c$$
$$\forall dw, t_\tau \in g_\tau \qquad (1)$$

In which $\hat{Z}_k$ is the maximum value of Z_k, $\bar{Z}_k$ the mean, σ the standard deviation, $\text{card}(\cdot)$ the cardinal operator and g_τ the original time series bucketed by τ. c is a coefficient that assumes significance in upper-bound estimation, being set at 1.5. This value was determined through empirical testing, that is, the value that minimized the RMSE metric, given the range $[1.1, 2]$.

For each date-time bucket (d, t_τ), the Power Spectral Density (PSD) S_{zz} is calculated. Our goal is to highlight the set of frequencies that most contribute to the S_{zz} peaks, so we compute the covariance matrix $\Sigma_{\tilde{Z}_\kappa, S_{zz}}$ and compute its eigenvalues and eigenvectors. By scaling the eigenvectors by the eigenvalues, we obtain a vector subspace $W(v)$ indicating the main direction and magnitude of the contribution of $\tilde{Z}_\kappa$ to the S_{zz}. After calculating the centre $\overline{W}(v)$ of the vector subspace, we perform Density-Based Spatial Clustering of Applications with Noise (DBSCAN) on $\tilde{Z}_\kappa$ to find the subset of $\tilde{Z}_\kappa$ whose centroid is closest to $\overline{W}(v)$. The normalisation of $\tilde{Z}_\kappa$ to $W(v)$ is invariant due to the linearity of the transformation, so we keep the original value. On the selected cluster, we perform Kernel Density Estimation (KDE) to obtain an estimate of the probability density function of the anti-transformed values. The obtained density function is injected into the inspired particle filter to evaluate the posterior distribution of the particles in the time domain. particles are generated using a uniform distribution in the range defined by the minimum and maximum of the selected cluster. From the newly generated set of particles, those whose probability is above the user defined probability threshold are retained. For accuracy, the threshold should be specified in the neighborhood of 1, in order to select particles with high probability of being a correct prediction.

From these, the average is calculated as a result of the number of MAC-flap events expected for that time slot.

The details of the algorithm are presented in Algorithm 1.

1) Hyper-parameters: The following model input parameters can be tuned to adapt to various scenarios:

- ϵ' (DBSCAN):
  - This refers to the largest allowable distance between two samples, determining whether one sample is considered part of the neighborhood of the other.
- min-samples ms (DBSCAN):

Algorithm 1 Lachesis version 0

Require: $dw(d,t)$ ▷ Compute the weekday dw from the date d and time t
Require: $g(d,t)$ ▷ Compute the MAC-flap event numbers at date d and time t
Require: τ ▷ Time aggregation parameter, minute-based
Require: η ▷ Forecast flag
Require: ϵ ▷ Particle Filter probably threshold
Require: θ ▷ Number of particles
Require: ke, bw ▷ KDE kernel function, kernel bandwidth
Require: ϵ', ms ▷ DBSCAN Max. distance between samples, Min. number of samples
Ensure: $g(d,t) \geq 0$
  $g_\tau \leftarrow \{g(d,t)\}_\tau$ ▷ Sequence of $g(d,t)$ bucketed by τ
  $N \leftarrow 35$ ▷ Time window size in days
  $Y \leftarrow []$ ▷ Result
  if η is True **then**
    $c \leftarrow 1$ ▷ Forecast
  else
    $c \leftarrow 1.5$ ▷ Threshold prediction
  end if
  while $N > 0$ **do**
    $Z_\kappa \leftarrow \mathscr{F}[g_\tau]$ ▷ FFT
    $N \leftarrow N - 1$
  end while
  $\tilde{Z}_\kappa \leftarrow \left\lceil \left(\left(\sqrt{\hat{Z}_k} \cdot |\bar{Z}_k + 3\sigma| \right) + \sqrt{\mathrm{card}(Z_k)} \right) \cdot c \right\rceil_{\forall dw, t_\tau \in g_\tau}$
  $W \leftarrow 7$ ▷ Prediction timespan in days
  while $W > 0$ **do**
    $T \leftarrow \{t_\tau\}_\tau$ ▷ Time slot sequence
    while $|T| > 0$ **do** ▷ Sequence cardinality
      $S_{zz} \leftarrow \mathrm{PSD}(\tilde{Z}_\kappa)$
      $\Sigma_{\tilde{Z}_\kappa, S_{zz}} \leftarrow \mathrm{cov}(\tilde{Z}_\kappa, S_{zz})$
      $\zeta, \mathrm{v} \leftarrow \mathrm{eigen}(\Sigma_{\tilde{Z}_\kappa, S_{zz}})$
      $W(\mathrm{v}) \leftarrow \zeta \times \mathrm{v}$
      $C_\kappa \leftarrow \mathrm{DBSCAN}(\tilde{Z}_\kappa, \epsilon', ms)$
      $\tilde{C}_\kappa \leftarrow \arg\min(||C_\kappa - \overline{W}(\mathrm{v})||_2)$
      $\Upsilon_{\tilde{C}_\tau}(\tilde{C}_\tau) \leftarrow \mathrm{KDE}(\mathscr{F}^{-1}[\tilde{C}_\kappa], ke, bw)$
      $\Omega[\tilde{C}_\tau, \Upsilon_{\tilde{C}_\tau}(\tilde{C}_\tau), \theta]$ ▷ Particle Filter set
      $\Theta \leftarrow []$ ▷ Particles buffer
      for i in Ω **do**
        if $\Omega[i] \geq \epsilon$ **then**
          $\Theta \leftarrow \Omega[i]$
        end if
      end for
      $Y \leftarrow \overline{\Theta}$
      $|T| \leftarrow |T| - 1$
    end while
    $W \leftarrow W - 1$
  end while
  Return: Y

Algorithm 2 Lachesis version 1

  Variables: n, dw, t, η ▷ n nodes, dw weekday, t time, η forecast flag
Require: $Q \leftarrow \bar{q}(n, dw, t)$ ▷ Average of 4-weeks time series grouped by n, dw, t
Require: $S \leftarrow \bar{s}(n, dw, t)$ ▷ Average of 1-week time series grouped by n, dw, t
Require: $\hat{S} \leftarrow \hat{s}(n, dw, t)$ ▷ Prediction
  $Y \leftarrow []$ ▷ Result
Ensure: $Q \geq 0$
Ensure: $S \geq 0$
Ensure: $\hat{S} \geq 0$
  $\tilde{S} \leftarrow S - Q$
  $\sigma_{Q,S} \leftarrow \mathrm{cov}(Q, S)$
  $\phi \leftarrow 1 + \tilde{S}'$ ▷ $\tilde{S}'$ is the first derivative of $\tilde{S}$
  $\sigma_\phi \leftarrow \mathrm{std}(\phi)$
  $Y \leftarrow \left\lceil \hat{S} + \sqrt{\left| \phi \cdot \dfrac{\sigma_{Q,S}}{1 + \sigma_\phi} \right|} \right\rceil$
  $\alpha \leftarrow \left| \dfrac{||S - \hat{S}||_2 - \min(\hat{S})}{\max(S) - \min(\hat{S})} \right|$

  if η is True **then**
    $Y \leftarrow \left\lceil Y \cdot \left(1 + \dfrac{1}{\alpha}\right) \right\rceil$ ▷ Forecast
  else
    $Y \leftarrow \left\lceil Y \cdot \left(1 + \dfrac{\alpha}{10^{\lfloor \log_{10}|\alpha| \rfloor + 1}}\right) \right\rceil$ ▷ Threshold prediction
  end if
  Return: Y

D. Lachesis version 1

The second version of Lachesis requires a set of nodes for which a previous forecast $\hat{S}$ was generated using Lachesis v0 and data from the previous 4 weeks Q, of the 35-day historical period. In this second version, the system uses data from the last week S of the 35-day historical period, having the same date range as $\hat{S}$, to produce the forecast for the following week.

The premise of the model is to refine the time prediction by taking into account the deviation between S and $\hat{S}$, and between S and Q.

The coefficient used is the square root of the absolute value of the first derivative ϕ of the deviation between S and Q, multiplied by the ratio of the covariance $\sigma_{Q,S}$ to the standard deviation σ_ϕ (see Algorithm 2).

If the prediction flag η is set to true, the result is smoothed by α, *i.e.* the normalised Euclidean distance between $\hat{S}$ and S, otherwise by the ratio $\dfrac{\alpha}{10^{\lfloor \log_{10}|\alpha| \rfloor + 1}}$.

$\lfloor \log_{10}|\alpha| \rfloor + 1$ is the number of integer digits of α.

The details are described in the Algorithm 2.

V. EVALUATION

In this section, we benchmark Lachesis v0 and v1 against the models outlined in Section II based on the model development pipeline described in Section IV-A. The models are tuned based on an exploratory data analysis of the time series data, capturing the fundamental temporal characteristics of the data, including lags, periodicity, trend.

A. The First Glance

Figure 4 depicts an example of the prediction made by Lachesis v0 on a single node. The smoothed ground-truth trace

---

– This parameter specifies the minimum number of samples within a neighborhood.

- Kernel ke (KDE):

  – To be chosen from {"gaussian", "tophat", "epanechnikov", "exponential", "linear", "cosine"}.

- bandwidth bw (KDE):

  – The bandwidth of the kernel.

- θ: the number of particles to be generated by the inspired particle filter.

- ϵ: the probability threshold that a particle weight should exceed in order to be selected.

In our case we used the following values: $\epsilon' = 0.1$, $ms = 15$, $ke =$ "gaussian", $bw = 0.3$, $\theta = 100$, $\epsilon = 0.98$.

TABLE II Performance metrics of a balanced batch of nodes

Model	MSE	RMSE	MAE	Avg. Daily Alerted Nodes	Avg. Daily Alerts	Total Alerts
arima	1769.932±196.916	42.027±2.335	12.423±0.685	56.095±5.288	110.714±17.693	775±123.851
dlm	1769.038±612.300	41.622±7.418	11.907±2.629	71.381±6.671	158.571±18.548	1110±129.835
lachesis_v0	**4.990±0.227**	**2.234±0.051**	**1.184±0.018**	85.667±2.144	210.238±9.915	1471.667±69.407
lachesis_v1	3430.788±904.687	58.23±7.756	55.176±7.454	**15.048±4.908**	**33.333±15.369**	**233.333±107.584**
linear	1671.404±318.552	40.752±4.003	13.624±1.260	67.714±5.878	150.191±21.976	1051.333±153.832
phase1	15305014±6820400	3833.331±957.016	563.420±95.862	21.857±10.933	33.524±19.873	234.667±139.113
prophet	2353.651±886.237	47.953±9.014	14.039±2.876	65.476±6.118	135.524±16.993	948.667±118.951
quadratic	2018.9±93.3	44.924±1.044	14.43±1.273	66.905±7.593	140.619±20.991	984.333±146.937
sarima	4183.916±706.578	64.535±5.359	16.669±2.290	33.714±3.714	60.762±5.915	425.333±41.405

Model	t_train (s) / 1k data points	t_infer (s) / 1k data points	t_train (s) / 1k nodes	t_infer (s) / 1k nodes
arima	0.378±0.230	0.181±0.099	317.738±193.736	30.523±16.754
dlm	0.685±0.21	1.18±0.696	576.1±176.809	199.337±117.699
lachesis_v0	0.149±0.03	0.866±0.138	7508.336±1511.362	8734.203±1394.595
lachesis_v1	0.3995±0.107	**0.0005±0.0002**	20132.882±5398.693	5.1030±1.98
linear	0.0057±0.0031	0.03±0.015	4.8±2.567	5.065±2.48
phase1	**0.0025±0.0010**	0.043±0.013	**2.063±0.81**	7.297±2.126
prophet	0.27±0.06	0.756±0.229	228.916±50.335	127.78±38.72
quadratic	0.0055±0.0025	0.0298±0.0092	4.654±2.08	**5.033±1.554**
sarima	3.669±1.704	0.274±0.168	3085.996±1433.175	46.365±28.392

Model	TP	FP	TN	FN
arima	131.333±24.583	643.667±99.962	19366.667±187.431	6602.667±2978.339
dlm	**185.667±22.008**	924.333±109.441	18914±337.23	**6548.33±2949.41**
lachesis_v0	166±8.19	1305.667±64.933	14297±576.27	6568±2961.09
lachesis_v1	109±42.93	**124.33±73.078**	20154.667±240.80	6625±3008.168
linear	180.333±21.008	871±135.193	18823.667±296.659	6553.667±2970.17
phase1	61.333±11.930	173.333±135.711	**20293.667±204.962**	6672.667±2959.571
prophet	160.667±14.364	788±115.5	19118.33±287.77	6573.33±2952.52
quadratic	177.33±23.71	807±126.69	18951±424.72	6556.67±2953.11
sarima	97.33±3.79	328±37.8	19986±267.1	6636.67±2969.4

Model	accuracy	precision	recall	specificity	balanced accuracy
arima	0.734±0.078	0.169±0.008	0.023±0.012	0.968±0.005	0.495±0.004
dlm	0.724±0.081	0.167±0.007	0.0305±0.0110	0.953±0.006	0.492±0.006
lachesis_v0	0.654±0.0901	0.113±0.005	0.028±0.011	0.916±0.004	0.472±0.006
lachesis_v1	**0.7556±0.0819**	**0.4786±0.1171**	0.020±0.014	**0.9939±0.0035**	**0.5070±0.0056**
linear	0.7245±0.0762	0.172±0.011	**0.0305±0.0143**	0.956±0.007	0.4931±0.0043
phase1	0.7535±0.077	0.3096±0.1365	0.010±0.004	0.9916±0.0066	0.500±0.001
prophet	0.729±0.079	0.171±0.021	0.0264±0.0090	0.96±0.006	0.493±0.004
quadratic	0.73±0.08	0.18±0.01	0.029±0.012	0.959±0.007	0.494±0.005
sarima	0.748±0.080	0.2297±0.0141	0.016±0.007	0.984±0.002	0.5±0.003

functions as a reference for determining the precision of the prognosis. Since networking issues rarely happen, we create a balanced batch of nodes with and without networking issues to thoroughly benchmark various models in Section V-B. Then in Section V-C, we consider node batches clustered based on various temporal characteristics, namely stationarity, periodicity, and volatility.

B. A Balanced Batch of Nodes

We sampled 540 nodes to make predictions with the inference period spanned over 3 weeks, from "2023-06-25" to "2023-07-16". A balanced set of nodes was utilised, comprising of 138 nodes, of which 69 nodes experienced actual network issues, gathered through user feedback, and 69 nodes with no known history of network problems. The previous 5 weeks were used as the training set. In Lachesis v1, the fifth week's historical data is used as the prediction basis, building on Lachesis v0's results. The results are shown in Table II.

The findings indicated improved precision on the Lachesis v0 regression metrics and the number of triggered alerts. However, with respect to the confusion metrics, there is a small reduction in the Lachesis v0 model's accuracy in comparison to DLM on true positives and false negatives. Conversely, Lachesis v1 shows the lowest outcomes in false positives prediction, surpassing all other models. As for true negatives, Lachesis v1 slightly surpasses phase 1. Lachesis v1 illustrates
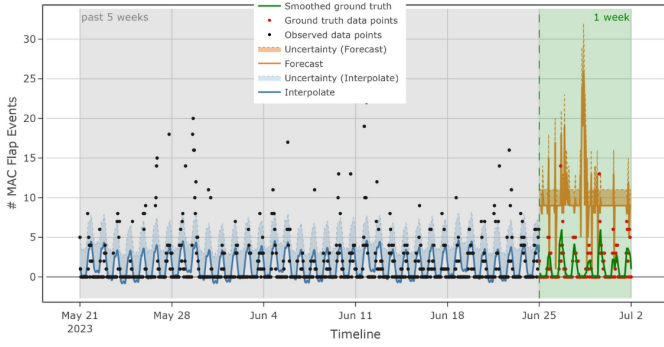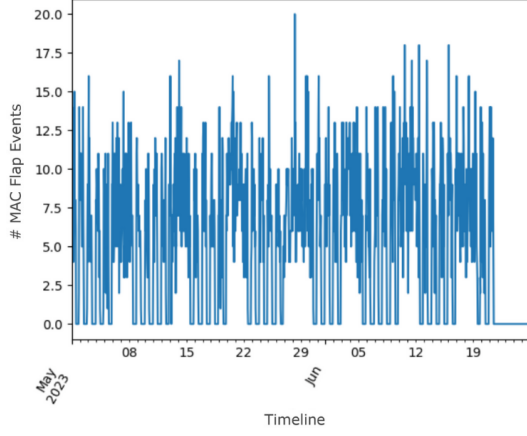
Fig. 4. Lachesis v0 prediction

Fig. 6. Volatility: an example of a time series classified as highly volatile

Fig. 5. Stationary: an example of a time series classified as high stationary

Fig. 7. Periodicity: an example of a time series classified as highly periodic

the highest precision and accuracy.

C. Node Batches Clustered on Temporal Characteristics

An initial data preparation phase is required to cluster nodes based on time series properties, namely stationarity, periodicity and volatility.

1) Stationarity: The stationarity is determined based on both the Kwiatkowski-Phillips-Schmidt-Shin (KPSS) test [25] and the mean-variance deviation test. High stationarity is determined following a total agreement of both the tests. Figure 5 shows an example of node with a high stationary time series.

2) Volatility: Let H be a single node time series, volatility is evaluated as follows

$$\nu = \text{std}\left(\frac{d(\ln[H+1])}{dt}\right) \cdot \sqrt{\text{card}\left(\frac{d(\ln[H+1])}{dt}\right)} \quad (2)$$

Clusters are formed using a K-means clustering algorithm on ν values and nodes are labelled as *high*, *medium* and *low*. Figure 6 shows an example of node experiencing a *high* volatility time series.

3) Periodicity: A customized formula has been designed to assess the recurrence of MAC-flap events on the same day of the week and time of day. This is to evaluate the underlying assumption of the Lachesis model, that anomalies due to non-malicious causes recur consistently on the same day
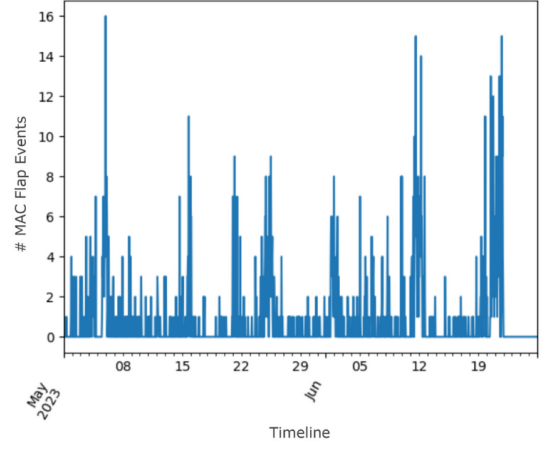
of the week and time of day, whereas malicious anomalies are associated with sporadic occurrences.

$$\text{R}_{dw,t_\tau} = \frac{1}{1 + 2\sigma' \mathbb{P}_{dw,t_\tau}(mode)} \quad \forall dw, t_\tau \in H_\tau \quad (3)$$

with

$$\mathbb{P}_{dw,t_\tau}(mode) = \frac{\max_{o \in O}(f_o)}{\sum_{o \in O} f_o} \quad (4)$$

such that O is the set containing the size of events, in terms of number of alerts, and f_o is the relative frequency of occurence. Figure 7 shows an example of node experiencing a highly periodic time series.

4) Results: A group of nodes was analysed, with 71 being classified as having *high* stationarity, 105 demonstrating *high* periodicity, and 21 nodes exhibiting *high* volatility. The inference period lasted for one week, between "2023-06-25" and "2023-07-02".

The assessment primarily focused on the regression and alerting accuracy, as the computational complexity over time had been previously evaluated. Therefore, an expanded version of these metrics is presented in Tables III-V.

The findings revealed that Lachesis v0 exhibited consistent leadership on the regression metrics across all three clusters,

TABLE III Performance metrics of a batch of nodes with high periodicity

Model	MSE	RMSE	MAE	Avg. Daily Alerted Nodes	Avg. Daily Alerts	Avg. Alert duration (min.)	Std. Alert duration (min.)	Avg. Alerts per hour	Std. Alerts per hour
arima	181.675	8.116	4.330	53.3	111.3	110.76	100.127	4.726	2.708
dlm	212.795	9.207	5.590	64.2	143.5	108.68	105.475	6.021	2.869
lachesis_v0	**1.441**	**1.143**	**1.003**	76.3	188.5	217.37	311.608	7.854	3.491
lachesis_v1	2384.963	48.532	48.052	**8.8**	**16.3**	101.44	**69.968**	**1.468**	**0.889**
linear	176.812	8.492	5.182	64.0	151.3	121.16	123.672	6.369	3.020
phase1	9280.777	42.813	19.870	30.2	49.5	**96.98**	77.192	2.753	1.656
prophet	200.930	8.954	5.729	59.2	128.8	109.34	95.463	5.496	2.708
quadratic	217.408	9.319	6.372	61.7	136.0	114.34	111.667	5.693	3.068
sarima	303.269	9.430	5.714	33.0	56.8	103.73	96.163	2.684	1.635

Model	TP	FP	TN	FN	accuracy	precision	recall	specificity	balanced accuracy
arima	88	580	17153	152	0.959	0.132	0.367	0.967	0.667
dlm	97	764	16835	**122**	0.950	0.113	**0.443**	0.957	**0.700**
lachesis_v0	69	1062	14341	306	0.913	0.061	0.184	0.931	0.558
lachesis_v1	44	**54**	**18198**	284	**0.982**	**0.449**	0.134	**0.997**	0.566
linear	**101**	807	16562	139	0.946	0.111	0.421	0.954	0.687
phase1	33	264	17822	538	0.957	0.111	0.058	0.985	0.522
prophet	76	697	16955	171	0.952	0.098	0.308	0.961	0.634
quadratic	92	724	16829	147	0.951	0.113	0.385	0.959	0.672
sarima	54	287	17776	268	0.970	0.158	0.168	0.984	0.576

TABLE IV Performance metrics of a batch of nodes with full stationary

Model	MSE	RMSE	MAE	Avg. Daily Alerted Nodes	Avg. Daily Alerts	Avg. Alert duration (min.)	Std. Alert duration (min.)	Avg. Alerts per hour	Std. Alerts per hour
arima	3103.485	28.589	20.025	38.667	86.167	**102.180**	**83.891**	3.743	1.874
dlm	4180.125	31.871	23.351	47.333	111.167	105.361	100.870	4.663	2.320
lachesis_v0	**8.148**	**1.857**	**1.339**	54.167	142.667	307.934	437.898	5.975	3.029
lachesis_v1	2630.949	49.714	47.448	**19.833**	50.833	144.803	174.928	2.584	1.420
linear	3074.893	29.547	22.516	47	120.333	120.445	118.650	5.159	2.447
phase1	13406608.127	1003.923	789.627	22.667	**36.500**	109.924	94.509	**2.229**	**1.316**
prophet	5826.676	35.251	26.949	45	101.500	110.972	103.088	4.374	2.071
quadratic	3484.138	30.256	23.721	45.667	105.667	110.347	106.205	4.584	2.192
sarima	6604.831	38.787	29.096	25.333	45	113.333	104.820	2.390	1.348

Model	TP	FP	TN	FN	accuracy	precision	recall	specificity	balanced accuracy
arima	117	400	17243	1530	0.900	0.226	0.071	0.977	0.524
dlm	136	531	16970	1401	0.899	0.204	0.088	0.970	0.529
lachesis_v0	114	742	13879	1245	0.876	0.133	0.084	0.949	0.517
lachesis_v1	126	179	17396	1101	**0.932**	**0.413**	0.103	0.990	0.546
linear	**150**	572	16713	**925**	0.918	0.208	**0.140**	0.967	**0.553**
phase1	46	**173**	**17616**	2604	0.864	0.210	0.017	**0.990**	0.504
prophet	108	501	16983	1919	0.876	0.177	0.053	0.971	0.512
quadratic	138	496	16983	1192	0.910	0.218	0.104	0.972	0.538
sarima	72	198	17576	2179	0.881	0.267	0.032	0.989	0.510

surpassing the performance of the other models. However, v1's primate on the alertness and confusion metrics is only sustained within the periodic cluster, aligning with the Lachesis grounded hypothesis, as illustrated in Table III.

Under the assumption of complete stationarity, the phase 1 model exhibited the best overall performance regarding confusion and alerting metrics. Both versions of Lachesis demonstrated strong results compared to the other models, particularly maintaining a leadership position in terms of accuracy and precision metrics, see Table IV.

In the volatility cluster, SARIMA exhibited the best performance in terms of daily alarms as well as the metrics for alarm duration and false positive predictions. Nonetheless, Lachesis v1 outperformed all models in terms of true positive detection and overall user experience related metrics, with

Linear Regression coming in second place as shown in Table V.

VI. CONCLUSION

In this paper, we proposed a systematic model development pipeline, which embraces a holistic approach that accords equal primacy to technical prowess and user experience metrics. Through the integration of user-centric feedback systems, our framework facilitates the seamless scaling of various models across diverse clusters of nodes, thereby enhancing evaluative precision and validation accuracy. This pipeline helped us develop an integrated anomaly detection system that employs a particle-filter-based algorithm named *Lachesis*. Results highlighted the superior forecasting capabilities of Lachesis v0 compared with existing models in literature,

TABLE V Performance metrics of a batch of nodes with high volatility

Model	MSE	RMSE	MAE	Avg. Daily Alerted Nodes	Avg. Daily Alerts	Avg. Alert duration (min.)	Std. Alert duration (min.)	Avg. Alerts per hour	Std. Alerts per hour
arima	8574.378	56.854	44.696	12.5	27.5	154.322	177.520	1.823	0.954
dlm	12175.386	65.003	50.037	14.5	31.5	118.017	102.821	1.765	0.964
lachesis_v0	**21.970**	**3.050**	**2.027**	16.833	41.333	396.687	536.435	2.167	1.411
lachesis_v1	3429.130	54	46.379	9.667	25.833	172.856	226.995	1.720	0.929
linear	8657.113	60.636	51.350	13.667	32	159.310	153.114	1.883	1.072
phase1	45179583.240	3128.713	2521.655	7.167	12.167	137.501	102.494	1.384	0.511
prophet	17761.725	76.574	61.494	15.167	31.500	139.667	130.948	1.759	1.049
quadratic	9752.012	58.776	49.066	14.5	32	132.414	125.119	1.893	1.090
sarima	19906.523	86.075	68.089	**6.667**	**10.833**	**107.337**	**78.960**	**1.232**	**0.407**

Model	TP	FP	TN	FN	accuracy	precision	recall	specificity	balanced accuracy
arima	33	132	17880	1331	0.924	0.200	0.024	0.993	0.508
dlm	46	143	17942	1222	0.929	0.243	0.036	0.992	0.514
lachesis_v0	56	192	16758	917	0.938	0.226	0.058	0.989	0.523
lachesis_v1	**59**	96	17905	841	0.950	**0.381**	**0.066**	0.995	**0.530**
linear	47	145	17807	**765**	**0.952**	0.245	0.058	0.992	0.525
phase1	21	52	18108	2015	0.898	0.288	0.010	0.997	0.504
prophet	37	152	17864	1701	0.906	0.196	0.021	0.992	0.506
quadratic	52	140	17899	999	0.940	0.271	0.049	0.992	0.521
sarima	22	**43**	**18176**	1876	0.905	0.338	0.012	**0.998**	0.505

while Lachesis v1 excelled in anomaly detection. Rigorous experimentation, which included scenarios concerning nodes affected by network issues, and clusters of nodes based on temporal characteristics, demonstrated the effectiveness of the two algorithms. This paper demonstrated the capacity of the proposed model development pipeline in enabling the efficient and continuous iteration of data-driven products, setting a new benchmark for responsive and user-centric anomaly detection systems.

REFERENCES

[1] N. Laptev, S. Amizadeh, and I. Flint, "Generic and scalable framework for automated time-series anomaly detection," in *Proceedings of the 21th ACM SIGKDD international conference on knowledge discovery and data mining*, 2015, pp. 1939–1947.

[2] O. Vallis, J. Hochenbaum, and A. Kejariwal, "A novel technique for long-term anomaly detection in the cloud," in *6th {USENIX} workshop on hot topics in cloud computing (HotCloud 14)*, 2014.

[3] Y. Zhao, S. Zhang, and Z. Yao, "A hybrid approach for smart alert generation," *arXiv preprint arXiv:2306.07983*, 2023.

[4] S. Omar, A. Ngadi, and H. H. Jebur, "Machine learning techniques for anomaly detection: an overview," *International Journal of Computer Applications*, vol. 79, no. 2, 2013.

[5] M. H. Bhuyan, D. K. Bhattacharyya, and J. K. Kalita, "Network anomaly detection: methods, systems and tools," *Ieee communications surveys & tutorials*, vol. 16, no. 1, pp. 303–336, 2013.

[6] M. Wang and S. Handurukande, "Anomaly detection for mobile network management," *INTERNATIONAL JOURNAL OF NEXT-GENERATION COMPUTING*, vol. 9, 01 2018.

[7] X. Chun-Hui, S. Chen, B. Cong-Xiao, and L. Xing, "Anomaly detection in network management system based on isolation forest," in *2018 4th Annual International Conference on Network and Information Systems for Computers (ICNISC)*, 2018, pp. 56–60.

[8] A. Dridi, C. Boucetta, S. E. Hammami, H. Afifi, and H. Moungla, "Stad: Spatio-temporal anomaly detection mechanism for mobile network management," *IEEE Transactions on Network and Service Management*, vol. 18, no. 1, pp. 894–906, 2021.

[9] R. Pan, X. Li, and K. Chakrabarty, "Semi-supervised root-cause analysis with co-training for integrated systems," in *2022 IEEE 40th VLSI Test Symposium (VTS)*, 2022, pp. 1–7.

[10] C. Kim, V. B. Mendiratta, and M. Thottan, "Unsupervised anomaly detection and root cause analysis in mobile networks," in *2020 Inter-national Conference on COMmunication Systems & NETworkS (COMSNETS)*, 2020, pp. 176–183.

[11] R. Pan, X. Li, and K. Chakrabarty, "Unsupervised root-cause analysis with transfer learning for integrated systems," in *2021 IEEE 39th VLSI Test Symposium (VTS)*, 2021, pp. 1–6.

[12] A. Gómez-Andrades, P. Muñoz, I. Serrano, and R. Barco, "Automatic root cause analysis for lte networks based on unsupervised techniques," *IEEE Transactions on Vehicular Technology*, vol. 65, no. 4, pp. 2369–2386, 2016.

[13] S. J. Taylor and B. Letham, "Forecasting at scale," *PeerJ Preprints*, vol. 5, p. e3190v2, 2017. [Online]. Available: https://doi.org/10.7287/peerj.preprints.3190v2

[14] https://facebook.github.io/prophet/docs/quick_start.html.

[15] M. West and J. Harrison, *Bayesian forecasting and dynamic models*. Springer Science & Business Media, 2006.

[16] https://pydlm.github.io.

[17] X. Jiang, S. Srivastava, S. Chatterjee, Y. Yu, J. Handler, P. Zhang, R. Bopardikar, D. Li, Y. Lin, U. Thakore, M. Brundage, G. Holt, C. Komurlu, R. Nagalla, Z. Wang, H. Sun, P. Gao, W. Cheung, J. Gao, Q. Wang, M. Guerard, M. Kazemi, Y. Chen, C. Zhou, S. Lee, N. Laptev, T. Levendovszky, J. Taylor, H. Qian, J. Zhang, A. Shoydokova, T. Singh, C. Zhu, Z. Baz, C. Bergmeir, D. Yu, A. Koylan, K. Jiang, P. Temiyasathit, and E. Yurtbay, "Kats," 3 2022. [Online]. Available: https://github.com/facebookresearch/Kats

[18] https://facebookresearch.github.io/Kats/api/kats.models.arima.html.

[19] https://facebookresearch.github.io/Kats/api/kats.models.sarima.html.

[20] https://scikit-learn.org/stable/modules/generated/sklearn.linear_model.LinearRegression.html#sklearn.linear_model.LinearRegression.

[21] https://scikit-learn.org/stable/modules/generated/sklearn.preprocessing.PolynomialFeatures.html.

[22] https://documentation.meraki.com/MS/Monitoring_and_Reporting/Loop_and_MAC_Flap_Detection_on_MS.

[23] https://documentation.meraki.com/MS/Port_and_VLAN_Configuration/Spanning_Tree_Protocol_(STP)_Overview#:~:text=Spanning%20tree%20protocol%20(STP)%20(,minute%20or%20more%20was%20acceptable.

[24] J. W. Cooley and J. W. Tukey, "An algorithm for the machine calculation of complex fourier series," *Mathematics of computation*, vol. 19, no. 90, pp. 297–301, 1965.

[25] D. Kwiatkowski, P. C. Phillips, P. Schmidt, and Y. Shin, "Testing the null hypothesis of stationarity against the alternative of a unit root: How sure are we that economic time series have a unit root?" *Journal of Econometrics*, vol. 54, no. 1, pp. 159–178, 1992. [Online]. Available: https://www.sciencedirect.com/science/article/pii/030440769290104Y